BRL MR 2249

BRL

MEMORANDUM REPORT NO. 2249

VACUUM ULTRAVIOLET RADIATION IN THE EXPANSION TUBE

by

Fritz H. Oertel, Jr.

November 1972

USA BALLISTIC RESEARCH LABORATORIES
ABERDEEN PROVING GROUND, MARYLAND

Destroy this report when it is no longer needed.
Do not return it to the originator.

Secondary distribution of this report by originating or sponsoring activity is prohibited.

Additional copies of this report may be purchased from the U.S. Department of Commerce, National Technical Information Service, Springfield, Virginia 22151

The findings in this report are not to be construed as an official Department of the Army position, unless so designated by other authorized documents.

B A L L I S T I C R E S E A R C H L A B O R A T O R I E S

MEMORANDUM REPORT NO. 2249

NOVEMBER 1972

VACUUM ULTRAVIOLET RADIATION IN THE EXPANSION TUBE

Fritz H. Oertel, Jr.

Exterior Ballistics Laboratory

RDT&E Project No. 1T061102A33D

A B E R D E E N P R O V I N G G R O U N D, M A R Y L A N D

B A L L I S T I C R E S E A R C H L A B O R A T O R I E S

MEMORANDUM REPORT NO. 2249

FHOertel/so
Aberdeen Proving Ground, Md.
September 1972

VACUUM ULTRAVIOLET RADIATION IN THE EXPANSION TUBE

ABSTRACT

The findings are presented of an optical survey of vacuum ultraviolet (VUV) radiation emitted from the shock layer of a 1-1/2" diameter sphere in hypersonic flows of air, argon, nitrogen and argon-nitrogen mixtures. Free stream velocities of 17,000 - 20,000 ft/sec and densities corresponding to altitudes ∿ 90,000 ft. were obtained in the BRL expansion tube facility; steady flow conditions prevailed over the model for about 75 μsec. The radiation was recorded on sensitized film down to a lower limit of 1100 Å. The purpose of the survey was to explore the feasibility of using this facility to measure time and space resolved radiation of the non-equilibrium, vibrationally-excited N_2 in the shock layer; part of this radiation is conjectured to ionize O_2 ahead of the shock around a hypersonic vehicle, thus enhancing its radar signature. Methods and problems of measuring VUV from this shock layer are discussed.

TABLE OF CONTENTS

LIST OF ILLUSTRATIONS

I. INTRODUCTION

Unexpected radar cross-section from ballistic reentry vehicles spurred interest in nonequilibrium radiation from the shock layer, especially the emission from vibrationally-excited nitrogen (N_2) in the Birge-Hopfield band system. This radiation can photoionize oxygen (O_2) ahead of the bow shock wave causing an electron field which influences a tracking radar return signal.

This problem has been studied in the laboratory by exciting vibrational energy levels behind normal shock waves propagating into N . Recent measurements of the spectral absorption coefficient in the Birge-Hopfield band system which extend below 1027 Å[1]*, the photoionization threshold of O_2 (Figure 1), overlaps earlier measurements at higher wavelengths[2]. Relating such absorption measurements to spectral emission presupposes local thermal equilibrium in the shock layer. In reality, the shock layer of a reentry vehicle is necessarily in a state of nonequilibrium since the Birge-Hopfield vibrational levels are energetically higher than the dissociation level of N_2. Consequently, it is important to simulate the actual case and to measure the spectrally-andspatially-resolved radiation emitted from the shock layer.

The purpose here is to report on equipment and procedures necessary to do an experiment in the troublesome vacuum ultraviolet (VUV) region of the spectrum, determine the impurities present in the expansion tube which may confound measurements of Birge-Hopfield emission, and establish procedures for recording VUV radiation on film. Having the latter capability is essential to making dynamic-shock, hook-fringe-interferometry measurements of oscillator strengths.

Impurity number density in the expansion tube has been measured previously[3]; however, these were in the visible region of the spectrum only. Many of the impurity elements commonly found in hypersonic flow facilities emit prominently in the ultraviolet. In addition, those measurements were pade prior to adopting the modified expansion tube mode of operation which eliminated mylar secondary diaphragms, a primary source of CN radiation.

II. APPROACH -- PROBLEMS IN THE VACUUM ULTRAVIOLET

Optical experiments in the ultraviolet region of the electromagnetic spectrum (approximately 200 - 3900 Å) impose rather stringent requirements on the experimenter (see for example a very complete review by Boyce[4]). In general, careful attention must be paid to absorption by the optical elements and by the intervening atmosphere.

References are listed on page 25.

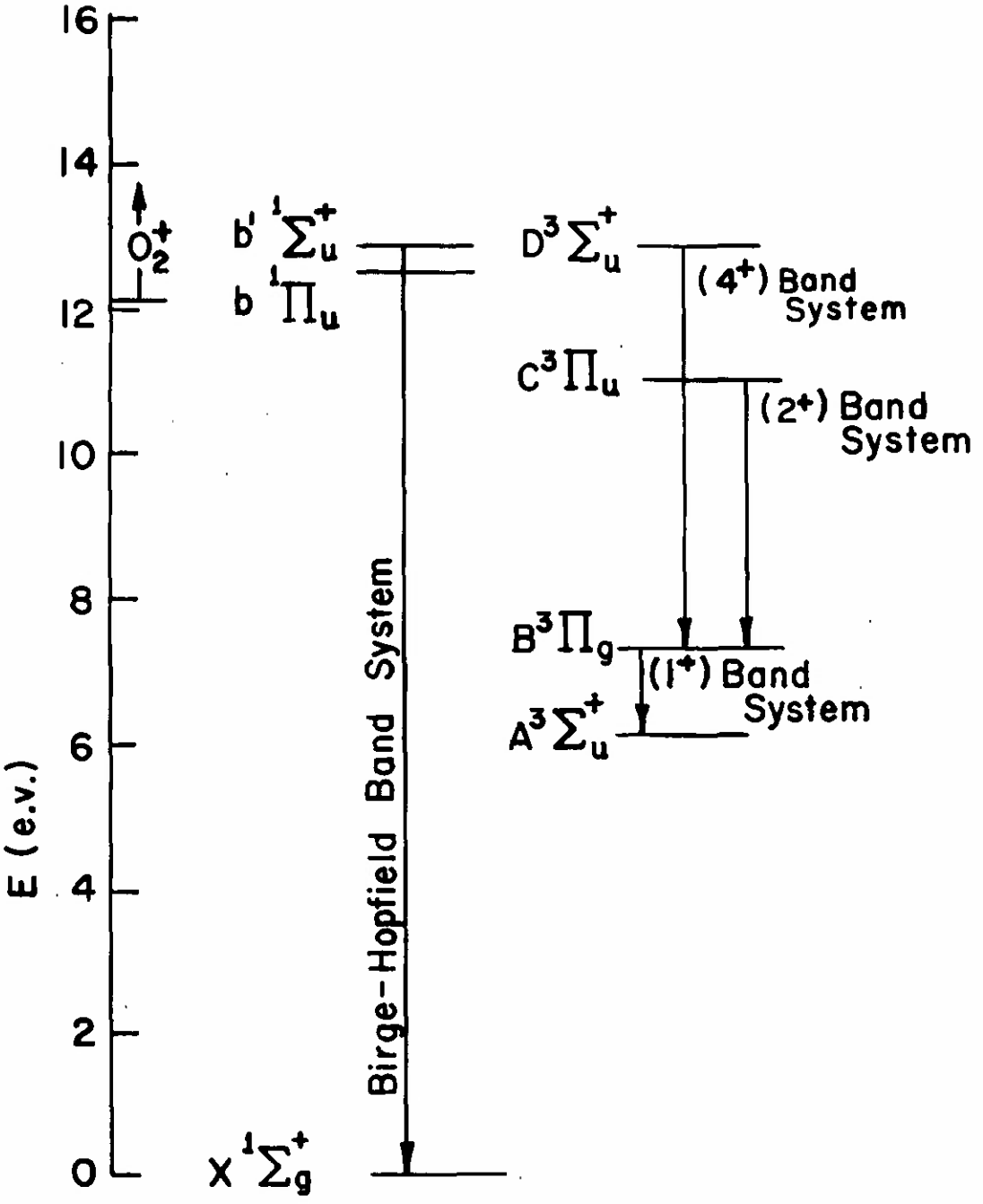

Figure 1. N_2 Energy Level Diagram

Below about 3400 Å most glass does not transmit. Indeed, in the wavelength region of interest, only magnesium fluoride (MgF_2) and lithium fluoride (LiF) transmit efficiently -- their respective lower transmission cutoffs are about 1150 Å and 1050 Å. LiF has the advantage of a lower cutoff level; however, it has the disadvantages of being hygroscopic (reacts with H_2O to form HF, an etching agent), and under prolonged exposure to intense UV radiation, its transmission degrades -- the cutoff shifts toward higher wavelength by as much as several hundred Å. Degradation is attributed to color-center formation in the material, a volume effect; however, it has been reported[2] that much of the original transmission can be restored by polishing. MgF_2 is much more chemically stable.

An additional restriction on optical components is imposed by decreased reflectivity of metallic surfaces with decreasing wavelength. For aluminum, which is widely used as a reflective coating, reflectivity decreases sharply below about 1800 Å. For new, clean aluminum surfaces, reflectance decreases nearly linearly with wavelength from about 0.80 at 1800 Å to about 0.10 at 1100 Å[5]. Reflectivity is further degraded by aging of the coating. Thin coatings of the reflecting surface with MgF_2 serve to protect the surface from abrasion and chemical action and increase the reflectivity. When several mirrors are to be used in an optical arrangement for the wavelength region around 1200 Å, they are normally over-coated with a layer of MgF_2 (or LiF) several hundred Å thick[5]. For a 3-mirror system, a gain in reflectivity by a factor of 30 can be realized. Such a gain can be significant at the low intensity levels normally measured in vacuum ultraviolet spectroscopy.

To perform an experiment at wavelengths below 2000 Å, where air absorbs strongly, the air in the optical path must be eliminated by evacuation or by purging with transparent gases such as helium (He). Between about 1750 Å and 1950 Å, absorption is due primarily to the Schumann-Runge band system of O_2. Merged with the band system is the strong Schumann-Runge continuum which extends to below 300 Å, with a transmission window between 1100 Å and 1300 Å[4]. Atmospheric nitrogen is completely transparent down to 1450 Å and absorbs only weakly down to LiF cutoff. It also has a transmission window between about 1100 Å and 1300 Å.

If the VUV radiation of interest is to be recorded photographically, specially-prepared films must be used. Special measures are necessary because the gelatin used as a binder of the photosensitive crystals begins to absorb strongly below 2265 Å. Commercial films with low gelatin content are available from several manufacturers for use throughout the vacuum ultraviolet. These films are very sensitive to abrasion and have a very slow photographic speed, ASA $\sim$ 50. As an alternative, strongly-fluorescing agents are commercially available which convert the UV radiation to the visible where fast, readily-available films with high photographic speeds (ASA $\sim$ 1250) may be used. Commercially-available sensitizing agents suffer from the disadvantage that a special

agent is needed to remove the sensitizer from the film prior to developing. Highly fluorescing oils, which are widely-used, also suffer from this disadvantage. Additionally, in a vacuum environment, the oil evaporates from the film resulting in decreased sensitivity, and, in all likelihood, would degrade performance of the optics by fouling. An attractive, readily-available sensitizer for the VUV is sodium salicylate. Dissolved in a solution of water and methyl alcohol it can be applied easily to the film surface. When applied properly, the solution dries quickly and will not soften the gelatin binder enough to cause it to crack upon drying. Consequently, the sensitized films are tough, relatively insensitive to abrasion, and can be subjected to vacuum conditions without harm to optical components and without loss of sensitivity. Sodium salicylate also has a nearly constant quantum efficiency over the entire UV wavelength region and fluoresces in the blue where many common films are sensitive. In addition, it is highly soluble in water and can be easily removed from the film prior to processing it in the usual manner.

III. EXPERIMENT

A. Experimental Apparatus and Technique

To generate the high-temperature, shock-layer flow, the BRL expansion tube[6], shown in schematic in Figure 2, was used. Steady, hypersonic, high energy flows of selected test gases, initially isolated in the driven section by the primary and secondary diaphragms, were generated by unsteady expansion to flow over a 1-1/2 inch diameter sphere model as shown in the lower portion of Figure 2. Free stream velocities were 17,000-20,000 ft/sec for densities known from other measurements to be comparable to the density at an altitude of $\sim$ 90,000 ft. Since only qualitative emission characteristics were of interest, no closer control of free stream conditions or measurement of them was necessary. Commercially-pure test gases used were: argon (Ar), nitrogen (N_2), and N_2 diluted with Ar (85% Ar: 15% N_2 by volume).

The experimental set-up is shown in Figure 3. The major component of the optical system, the Seya-Namioka vacuum monochromator[7] (spherical reflecting grating, 13 Å/mm, f/11) (Figure 4), was modified by a film-holder made with the film plane fixed tangent to the Rowland circle for specular reflection of the entrance slit image (so-called 0Å setting). Although the grating is used off the Rowland circle, the Seya-Namioka mount insures that the focus is on or very near the circle for the operating range of the instrument (0 Å - 4500 Å); thus the need for precise adjustment of the film plane location is relaxed.

The spectrograph was coupled to the expansion tube test section with a short section of flexible TYGON tubing and the entire volume up to the test section window was evacuated to $\sim$ 20 μHg. Lower vacuum levels were not necessary for this experiment. For this simple arrange-

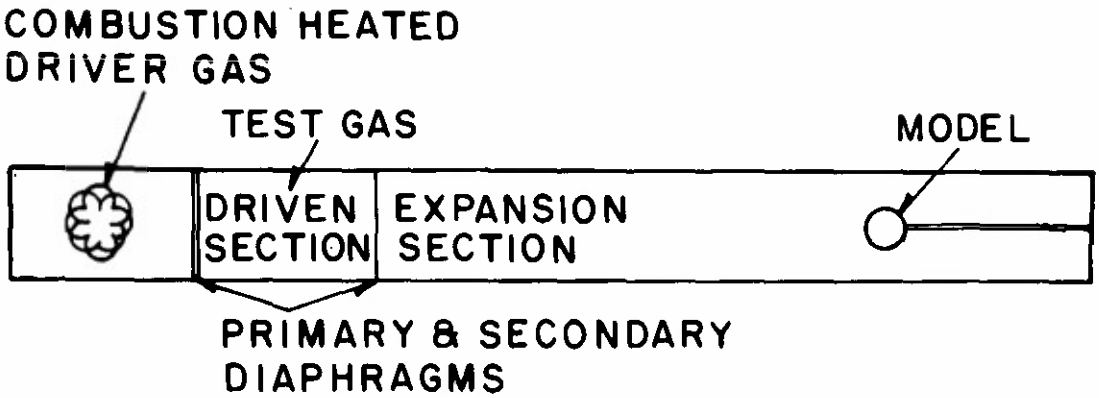

a. Schematic of Tube. Combustion Initiated Operation.

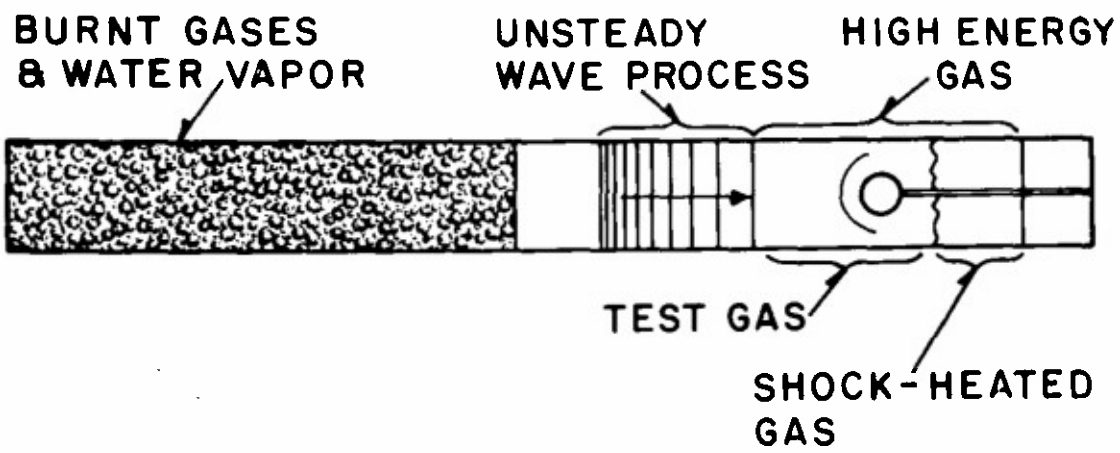

b. The Situation After a Shock Wave
Has Moved Into the Test Section.

Figure 2. Expansion Tube Operation

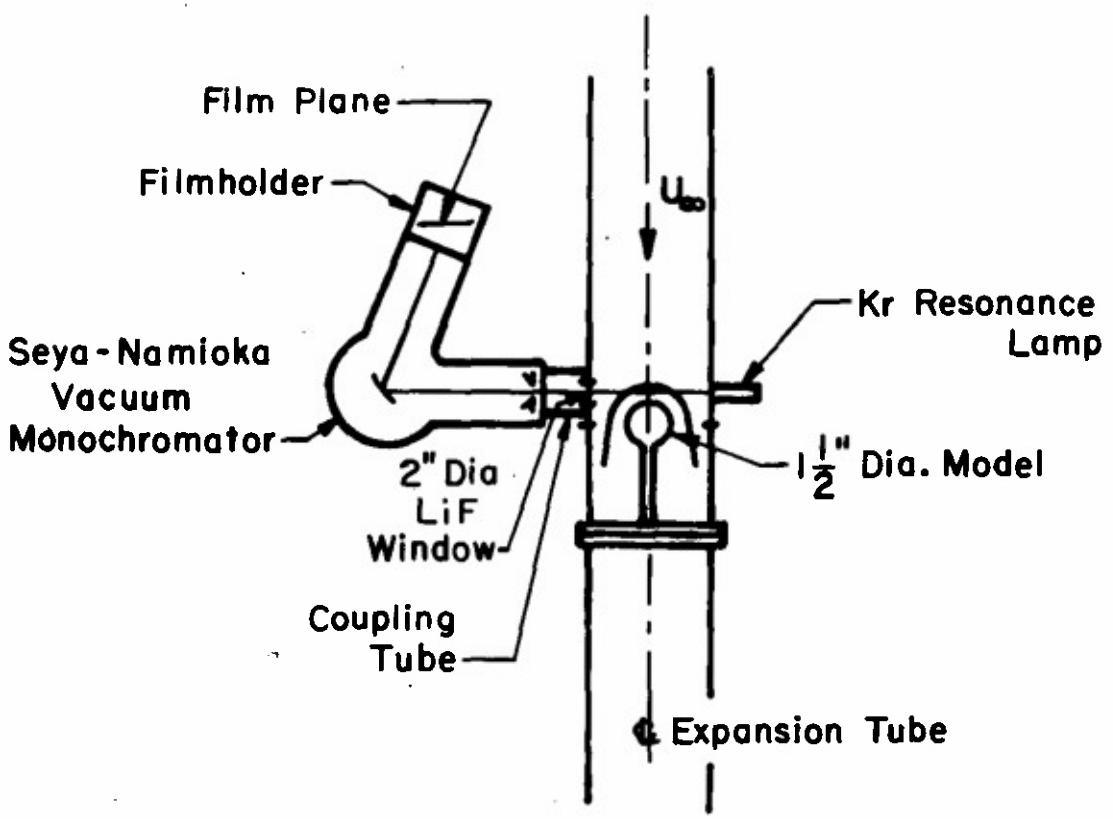

Figure 3. Experimental Set Up

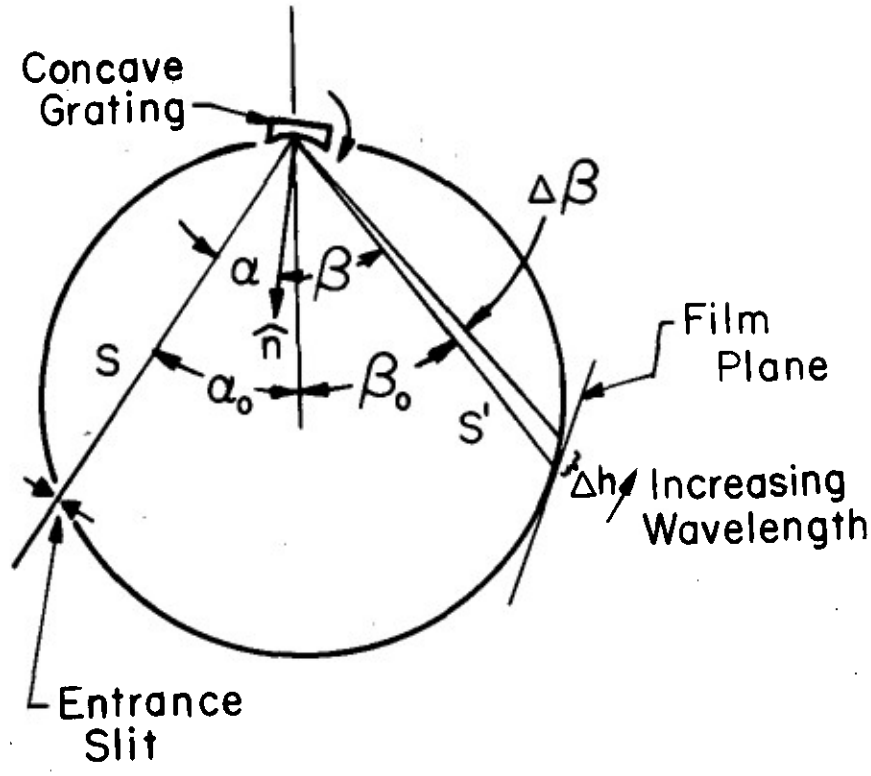

Figure 4. Seya-Namioka Monochromator

ment, the 1 cm thick LiF window and the MgF_2 over-coated concave grating were the only components in the optical train.

Since spatial resolution of the sphere's shock layer (see the discussion in Section III. B.) is not a factor in this experiment, radiation from the shock layer was not focused. Nor were spatially-separated slits placed along the line-of-sight to reduce the field of view of the grating. The field of view was controlled solely by the width of the spectrograph entrance slit and by the distance of the grating from the centerline of the test section. A region about 9/16-in. long was viewed on the axis of the model -- approximately a factor of four greater than the shock standoff distance for the conditions of the experiments. Large slit widths (100 - 200 μ) were used to admit as much radiation as possible.

For resolution of radiation from the shock layer, the use of a LiF lens would improve spatial resolution; and it would increase the intensity of light at the entrance slit of the spectrograph many-fold despite the loss due to transmission through an additional optical component.

B. Radiation Emitted in the Expansion Tube-Spectrograms

Time-integrated spectrograms were made of VUV radiation during runs in the expansion tube. Radiation was recorded on high speed film sensitized as described in Section II. Since no shutter is used, radiation from several causes may expose the film. An inspection of Figure 2 shows these possible causes and their order of occurrence from right-to-left as time passes: the residual air compression-heated by the shock wave which propagates into the partial vacuum of the expansion section after the secondary diaphragm opens; the high energy gas (shock-heated air and test gas) which is compression-heated in the bow shock of the model; and the products of the combustion driver. Making runs with, and without the model showed that the film was exposed only when the model was used. These results indicate that radiation prior to and following the flow of the test gas over the model does not expose the film. Several runs were also made with air in the spectrograph to check for ghosts; no exposure was seen. Hence, only VUV radiation exposed the film and it was emitted during the 50-100 μsec[6] the test gases and impurities flowed over the model. This radiation was emitted from the equilibrium and nonequilibrium regions of the shock layer.*

**For hypersonic flow past the model, the gases are first heated instantaneously in the compression shock and then relax to equilibrium in the shock layer. In general, equilibration proceeds according to the following ordering of relaxation times for translation, rotation, vibration, dissociation, and ionization:* $\tau_{trans} \sim \tau_{rot} < \tau_{vibr} < \tau_{diss} < \tau_{ioniz}$. *Since the vibrational energy levels of the Birge-Hopfield band system lie above the* N_2 *dissociation energy of 9.74 ev (see Figure 1), Birge-Hopfield emission is necessarily nonequilibrium emission.*

Spectrograms covering an interval from several hundred Å units below LiF cutoff to about 1800 Å (near air cutoff) were made for shock heated Ar, N_2, and Ar-N_2. This wavelength span allows impurity and other radiation of interest to be recorded and allows visual observation (down to LiF cutoff) of the region where one might make photometric measurements in the tail of the Birge-Hopfield band system. Weak lines on the film were seen when using the Ar-N_2 mixture; these are thought to be due to Birge-Hopfield and Lyman-Birge-Hopfield emissions[8]. However, these lines were not discernible at all when pure N_2 was used as test gas.

Sample spectrograms are shown in Figures 5 and 6. Noteworthy in these figures is the astigmatic image which is approximately 2.5 times the height of the entrance slit. This characteristic of the concave reflecting grating at large angles of incidence will be discussed in Section IV. Also noteworthy are the reference images from an electrodeless discharge lamp (see Figure 3) containing krypton (Kr) gas and trace amounts of carbon monoxide (CO). The Kr resonance lines, 1165 Å and 1236 Å, supplemented by prominent band heads of the fourth positive system of CO[9] (∿1450 Å - 1950 Å) provided a good light source for exploratory work in the VUV and known wavelengths for indexing the spectrograms.

IV. DATA REDUCTION AND DISCUSSION

A. Characteristics of the Seya-Namioka Grating Mount

Some of the results and conclusions of this work are seen more clearly in the light of the elementary theory of the spherical concave grating and its Seya-Namioka mount found in textbooks on experimental spectroscopy such as Samson[5] and Sawyer[10]. The theory of the concave grating has been treated in detail in papers by Beutler[11] and Namioka[7,12].

The Seya-Namioka monochromator is so constructed that: $\alpha_o=\beta_o=35^0$ 15' (Figure 4) and both slits lie on the Rowland circle. With the grating positioned so that $\alpha = \alpha_o$, light incident on the grating is reflected specularly and a white light image of the entrance slit is seen at the exit slit. This is the central image position. Due to the construction of the Seya-Namioka monochromator, the entrance slit remains focused at the exit slit within a fraction of a millimeter over the spectral range of the instrument (0 Å - 4500 Å). Beginning at the central image position (0 Å), this range is scanned during a 20^0 clockwise rotation of the grating about its axis (normal to the Rowland circle).

As mentioned earlier, the spherical concave grating mounted in this way has the optical aberration of astigmatism. That is, for a vertical entrance slit and vertical rulings, each object point on the illuminated entrance slit is imaged first as a vertical line and then as a horizontal line. Image distances for the concave reflecting grating (r' for

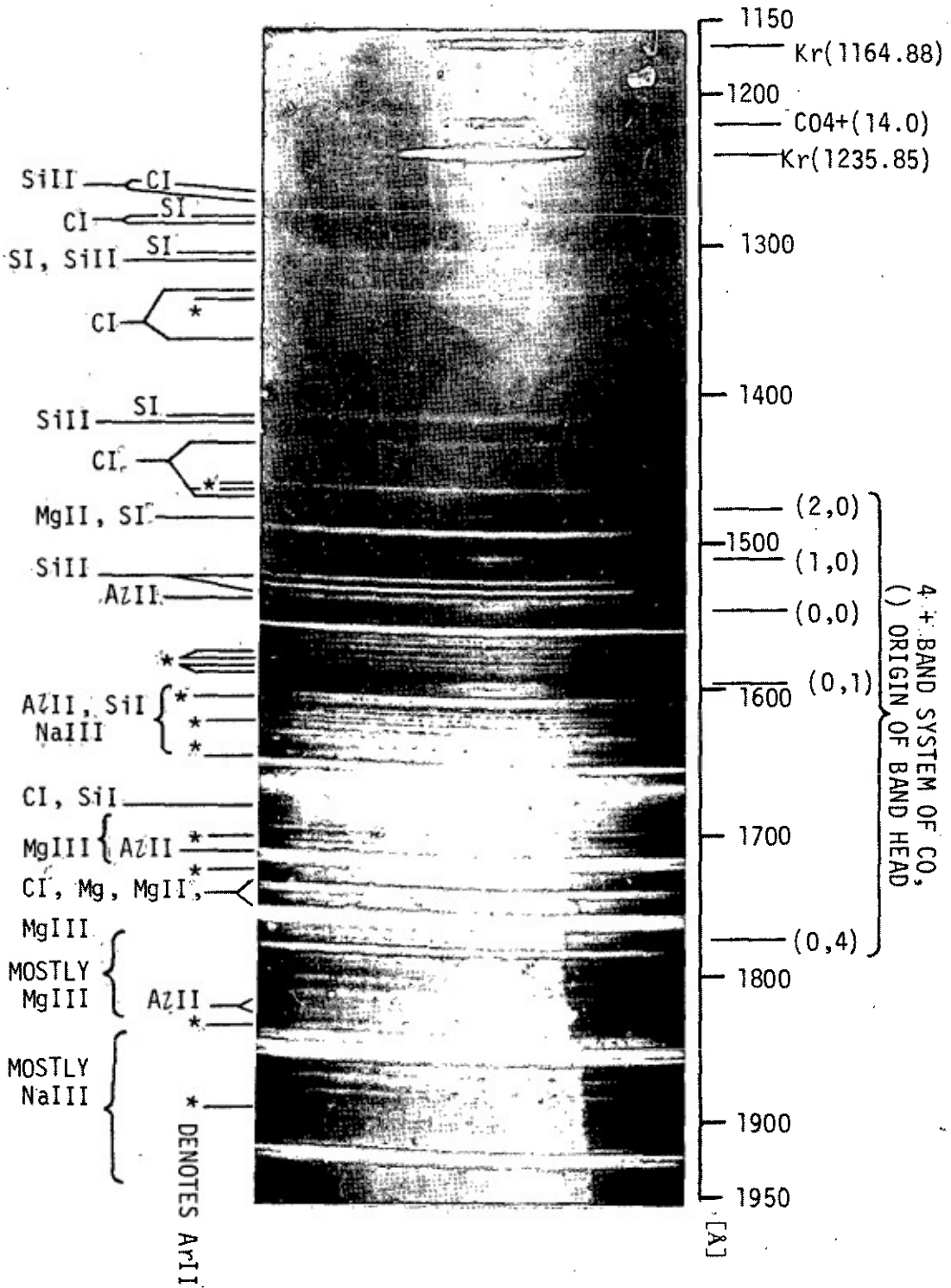

Figure 4. Spectrogram of VUV Emission from Shock-Heated Argon Spectrograph Entrance Slit 100 Microns.

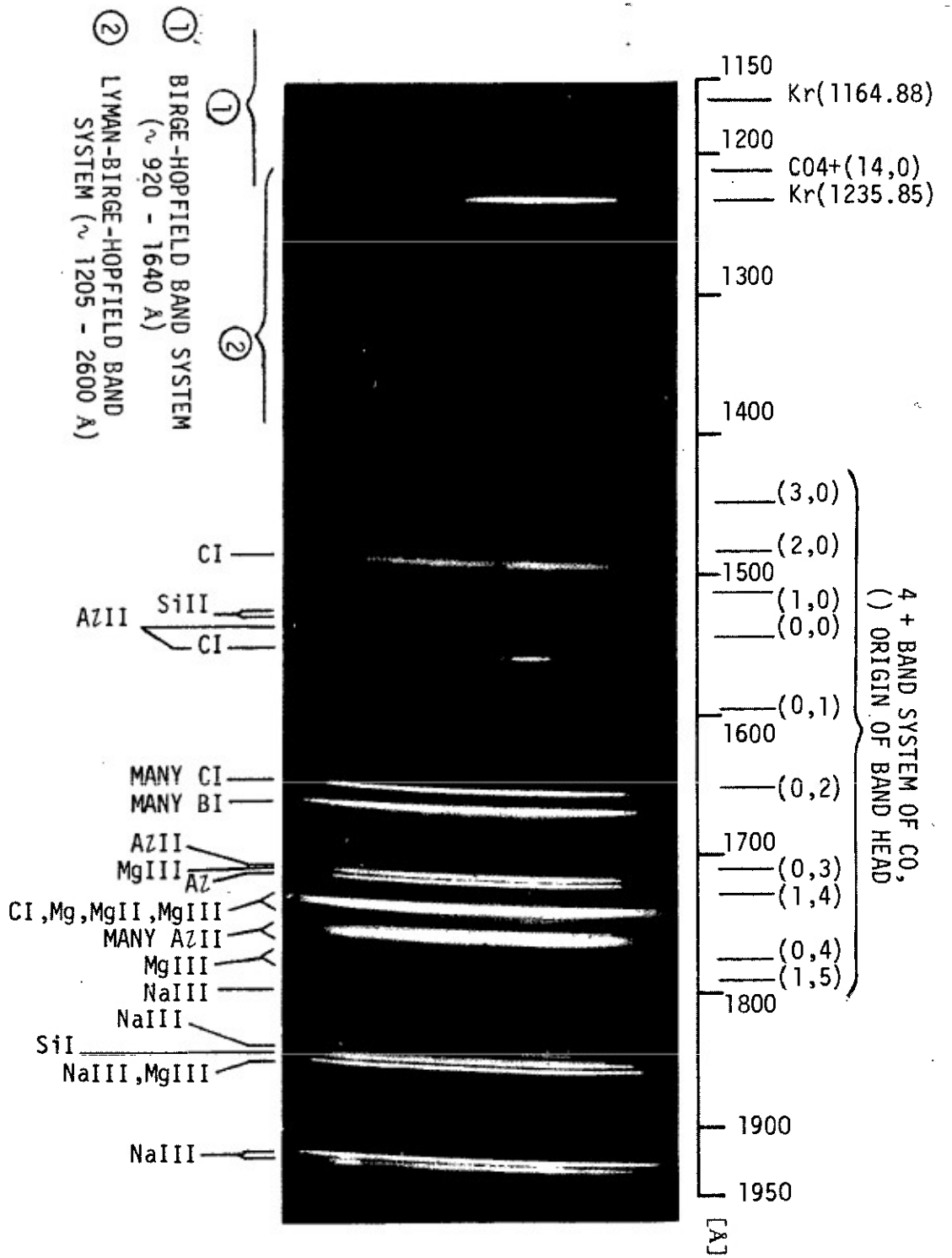

Figure 6. Spectrogram of VUV Emission from Shock-Heated Argon-Nitrogen Mixture. Spectrograph Entrance Slit 200 Microns.

the horizontal image and s' for the vertical image) are given in terms of the angles of incidence and dispersion, α and β respectively, and the object distance, s, by the astigmatic mirror equations

$$\left(\frac{\cos^2 \alpha}{s} - \frac{\cos \alpha}{R}\right) + \left(\frac{\cos^2 \beta}{s'} - \frac{\cos \beta}{R}\right) = 0 \qquad (1)$$

$$\left(\frac{1}{s} - \frac{\cos \alpha}{R}\right) + \left(\frac{1}{r'} - \frac{\cos \beta}{R}\right) = 0 \, . \qquad (2)$$

Here R is the radius of curvature of the concave grating. The horizontal image is located much farther from the grating than the vertical image used here.

Each astigmatic image is a superposition of the image lines. The horizontal image is very large and is generally not used. The vertical image has a total height given by

$$z = \ell \frac{\cos \beta}{\cos \alpha} + L\,[\sin^2\beta + \sin \alpha \tan \alpha \cos \beta] \, . \qquad (3)$$

Here ℓ is the length of the entrance slit and L is the length of the ruled lines illuminated. Astigmatic images are, in general, curved due to astigmatic curvature and enveloping curvature; and, for the most intense lines in this experiment, the curvature is accentuated by turbid exposure of the film. (See for example the strong 1236 Å Kr line relative to the weaker 1165 Å line.)

For this experiment, the monochromator was modified for use as a spectrograph as described in Section III. Examination of the spectrograms indicates that focus was satisfactory here over the full range of the film ($\sim$ 800 Å) for the monochromator so modified. Wavelength display on the film is governed by the grating equation.

$$\lambda = d/m\,[\cos \alpha + \cos \beta] \, , \qquad (4)$$

where λ is the wavelength of the dispersed light, d is the separation between adjacent rulings on the grating surface and the sign convention of a mirror is used for α and β. The plate factor for the grating -- the reciprocal linear dispersion (Å/mm) -- can be obtained by differentiating Eq. (4) for α = constant and assuming that $\nabla h = R\nabla\beta$ on the film (this condition holds on the Rowland circle) so that in the limit $d\lambda/dh = \cos \beta/[mR(1/d)]$. We see that the plate factor and wavelength both increase in the direction of the arrow in Figure 4. Clearly dispersion is nonlinear in β and is nearly linear only in the vicinity of the grating normal ($\beta \sim 0$). Although dispersion is a nonlinear function of β, it changes slowly for the spectral region of interest ($\beta \sim 50^o$). It was found that wavelengths could be determined to within a few Å units by fitting a linear dispersion to each 400 Å segment of the

spectrograms. However, wavelengths determined in this way were not accurate enough for our purposes and were used only for tentative identification.

B. Measurement of the Spectrograms

The spectrograms were read on an optical stereocomparator with an absolute accuracy of 10μ. Direct comparison of the spectrograms was not possible because of film stretching. However, stretching caused no Problem when determining the wavelength of unknown emissions since they were calculated by linear interpolation between closely-spaced reference wavelengths. This method of reduction yielded unknown wavelengths accurate to tenths of an Å unit.*

Initially only the Kr resonance lines were known. Later, the other reference emissions were identified, at first tentatively by the linear dispersion relation mentioned in the previous section, then more positively by the manufacturer's disclosure that CO contamination of the Kr gas occurs with use. The CO is apparently a residual from manufacture of the lamp's glass envelope. Emissions are from its fourth positive band system, the ground state transition $A\ ^1\pi \leftrightarrow X\ ^1\Sigma^+$. Most of the listed band heads were observed on other films using the calibration lamp. Band structure degraded to the red was seen for an older, more contaminated lamp. Several of the more prominent band heads can be seen in Figures 5-6 -- the origin of the heads are indicated in parentheses. Others are not visible on these reproductions. Since the lamp was farther from the grating these reference images are shorter.

Knowing these reference wavelengths, a wavelength was computed for the other emissions seen on the spectrograms by linear interpolation, which is certainly valid for short wavelength intervals. The wavelengths determined in this manner were then compared with known wavelengths listed in tables of emission characteristics[13-15] for identification with a particular element. In this way, the lamp's reference wavelengths were augmented by several impurity lines for which identification was considered positive; for example, most emissions characteristic of SiII and CI were found (see Figures 5 and 6) -- several of them listed as persistent-- while only a few were obscured by emissions from other elements. (I, II, etc. designate an element's atom, first ion, etc.) From this smaller wavelength interval of precisely-known wavelengths, more impurity lines could be identified and possible impurity elements investigated; e.g., those associated with the windows (B, Si, Li, F, Mg, etc.); common to the walls and diaphragms; and other sources such as pump oils, and cleaning materials and agents. Several of these impurities were also found in shock tube experimentation[16].

**This accuracy is based on constant reading error from line-to-line for the same observer. It may not be valid for the more intense lines -- see discussion after Eq. (3), Section IV.A.*

Despite the small separation between wavelengths used for reference, identification of some of the wavelengths with an emitter is uncertain for two reasons. First, wavelength data are scarce and not as accurately measured in the VUV. The scarcity of data can be attributed to the difficulty of working in the VUV. Accuracy of wavelength measurement -- often no better than several tenths of an Å unit -- is mainly limited by the physical size of vacuum spectrographs relative to those used for measurements in the visible spectrum. Second, several elements known to be possible impurity elements may emit in a wavelength interval within the accuracy of the wavelength determination. Although it is unlikely that all listed emissions for an element will be obscured by other emissions, positive identification cannot be made when only a few characteristic wavelengths are observed.

In addition to the impurity emissions mentioned above, it is felt that ion emissions for ArII, AlII, Mg III, and NaIII were positively identified. Other possible emitters which were less positively identified are shown on Figures 5 and 6; others are: Al, Ar, Fe, FeII, LiII, and CaII. A few emissions were not identified, perhaps because spectral emission tables for the VUV are scarce or incomplete.

Of the elements considered in the original expansion tube[3] only iron (Fe) and the iron ion (FeII) were identified, but not conclusively since several emissions which would not be obscured by other radiation were not seen. This leaves unsubstantiated the assumption of high iron ion concentration used in estimating impurity number density in Reference 3. No conclusions regarding chromium can be drawn because only states too energetic for this shock-heating mode of excitation (doubly and triply ionized Cr) fall in the wavelength interval of these spectrograms. CN radiation, prominent in Reference 3, may have been seen here in the $J\ ^2\Delta_i \rightarrow A\ ^2\pi_i$ system, however, other radiation coincided with each band head precluding more positive identification.

The regions of interest for photometric measurements are indicated on Figure 6; they are the Birge-Hopfield band system of N_2 (above LiF cutoff) and its less energetic Lyman-Birge-Hopfield band system. Film exposure seen within the bracketed regions could not be identified with impurities. Exposure due to this radiation like some of the other weak exposures can only be seen on the original films.

It was observed on several films that the intensity was consistently greater when pure Ar was used. This result should be expected for the same flow conditions since the temperature of the purely monatomic test gas is expected to be higher. In the Ar-N_2 gas mixture, energy goes into exciting and dissociating N_2 molecules. As a result of the higher temperature, the intensity of radiation from the ionized species should be greater.

V. SUMMARY AND CONCLUSIONS

Spectrally-resolved radiation from shock-heated gases has been recorded photographically in the vacuum ultraviolet region of the spectrum from LiF cutoff to beyond air cutoff on high speed film sensitized with sodium salicylate. Sodium salicylate is widely used as a wavelength converter, but its role as a film sensitizer has not been emphasized.

One of the possible disadvantages of this combination, especially for applications such as interferometry, is that the sensitizer/high speed film combination has lower resolution than slower films. However, for this experiment, it was found that the photographic speed of conventional high resolution films for this spectral region was too low. Since energy densities in this experiment are higher and exposure times (50-100 μsec) longer than those available for photography of a dynamic shock wave, concessions must be made to accept lower resolution. In addition, a very high intensity continuum backlight is indicated and all optics must be coated for efficient reflection in this spectral region.

The astigmatic image formed by the Seya-Namioka instrument is not detrimental for photometric measurements, especially if the slit height and illuminated height of the grating are kept small (see Eq. (3)).

For hook-fringe interferometry, image quality is important. If an interferometer were optically-coupled to the Seya-Namioka spectrograph, fringes from the interferometer, focused at the spectrograph's entrance slit, normal to the slit jaws, would not be preserved in the exit plane of the vertical astigmatic image because of image overlap (see earlier discussion in Section IV). Fringes would be preserved for the horizontal image, but since spectral range is very limited and the image distance is large (see Eq. (2)) -- both conditions dictating a very large evacuated film box -- this possibility is primarily of academic interest.

The total impurity level for the expansion tube appears to be on the order of one hundred parts per million for both the unmodified[3] and modified[17] operating cycles, although relative concentrations of the impurities appear to be different. In the modified expansion tube, Spurk and Gion[3] reported that iron, chromium, and CN emissions were all less intense than those recorded in the original expansion tube. However, in the original cycle, CN radiation was quite prominent, because Mylar secondary diaphragms were used. In this experiment, aluminum atom and ion emissions were prominent since the secondary diaphragms were made of aluminum.

Since photomultiplier measurements are orders of magnitude more sensitive than the film, it is important to identify the areas in the region of interest where impurities do not emit. Based on the findings of these experiments, it appears that unambiguous photometric measurements can be made for Birge-Hopfield radiation above LiF cutoff for the conditions described.

The absence of lines between LiF cutoff and $\sim$ 2000 Å for tests in pure N_2 is a little surprising. It may only be concluded that N_2-N_2 collisions have a different efficiency and overall effect on the relaxation of N_2 than do Ar-N_2 collisions. [Rate constants for these reactions are not very well known.] In addition, the absorption characteristics of the pure N_2 shock layer are evidently quite different, since impurity emissions, which were seen at the higher wavelengths for both the Ar and Ar-N_2 runs, were not seen for pure N_2 runs at the same initial conditions. However, it should be remembered that the situation is complicated in each case by a different initial shocked-gas temperature, in addition to different dominant collision partners.

Atom and first ion emissions from argon have also been identified in this region. These high energy transitions, normally not included in computation of high temperature indices of refraction, internal partition functions, and radiative heat transfer, can have a noticeable effect[18]. This situation exists because experimental data -- even wavelength data for common elements -- are scarce in this spectral region. Many tabulated wavelengths are computed from isoelectronic sequences.

REFERENCES

1. W. H. Wurster, "Precursor Ionization from Blunt Body Shock Waves," CAL No. AF-2851-A-2, July 1970, Cornell Aeronautical Laboratory, Buffalo, N. Y.

2. J. P. Appleton and M. Steinberg, "Vacuum-Ultraviolet Absorption of Shock-Heated Vibrationally Excited Nitrogen," J. Chem. Phys., Vol. 46, No. 4, pp. 1521-1529, February 1967.

3. J. H. Spurk and E. J. Gion, "Impurity Concentration in the Expansion Tube," AIAA Journal, Vol. 7, No. 2, pp. 346-348, February 1969, and Ballistic Research Laboratories Report 1404, AD 673109, June 1968.

4. J. C. Boyce, "Spectroscopy in the Vacuum Ultraviolet," Rev. Mod. Phys., Vol. 13, No. 1, pp. 1-57, January 1941.

5. J.A.R. Samson, Techniques of Vacuum Ultraviolet Spectroscopy, John Wiley and Sons, Inc., New York, 1967.

6. J. H. Spurk, E. J. Gion, and W. B. Sturek, "Modified Expansion Tube," AIAA Journal, Vol. 7, No. 2, February 1969, pp. 345-346, and Ballistic Research Laboratories Report 1404, AD 673109,June 1968.

7. T. Namioka, "Theory of the Concave Grating, III. Seya-Namioka Monochromator," J. Opt. Soc. Am., Vol. 49, No. 10, October 1959, pp. 951-961.

8. L. Wallace, "A Collection of the Band-Head Wavelengths of N_2 and N_2^+," The Astrophysical Journal, Supplement No. 62, Vol. VI, February 1962, pp. 445-480.

9. L. Wallace, "Band-Head Wavelengths of C_2, CH, CN, CO, NH, NO, O_2, OH, and Their Ions," The As rophysical Journal, Supplement No. 68, Vol. VII, October 1962, pp. 165-290.

10. R. A. Sawyer, Experimental Spectroscopy, Dover Publications, Inc., New York, 1963.

11. H. G. Beutler, "The Theory of the Concave Grating," J. Opt. Soc. Am., Vol. 35, No. 5, May 1945, pp. 311-350.

12. T. Namioka, "Theory of the Concave Grating," J. Opt. Soc. Am., Vol. 49, No. 5, May 1959, pp. 446-465.

13. R. L. Kelly, "Atomic Emission Lines Below 2000 Angstroms - Hydrogen Through Argon," NRL Report 6648, February 1968, Naval Research Laboratory, Washington, D. C.

14. H. Kayser, Tabelle der Hauptlinien der Linienspektren aller Elemente nach Wellenlänge geordnet, Julius Springer Verlag, Berlin, 1939.

15. R. W. B. Pearse and A. G. Gaydon, The Identification of Molecular Spectra, John Wiley and Sons, Inc., New York, 1950.

16. H. E. Petschek, P. H. Rose, H. S. Glick, A. Kane, and A. Kantrowitz, "Spectroscopic Studies of Highly Ionized Argon Produced by Shock Waves," J. Appl. Phys., Vol. 26, No. 1, pp. 83-95, January 1955.

17. F. H. Oertel, "Measurement of Electron Concentrations in Axisymmetric Nonequilibrium Shock Layer," Ballistic Research Laboratories Report 1594, AD 748833, June 1972.

18. K. H. Horn, H. Wong, and D. Bershader, "Radiative Behavior of a Shock-Heated Argon Plasma Flow," J. Plasma Phys., Vol. 1, No. 2, pp. 157-170, 1967.

DISTRIBUTION LIST

No. of Copies	Organization
12	Commander Defense Documentation Center ATTN: TIPCR Cameron Station Alexandria, Virginia 22314
1	Director Defense Nuclear Agency Washington, D.C. 20305
1	Commander U.S. Army Materiel Command ATTN: AMCDL Washington, D.C. 20315
1	Commander U.S. Army Materiel Command ATTN: AMCRD, Dr.J.V.R.Kaufman Washington, D.C. 20315
1	Commander U.S. Army Materiel Command ATTN: AMCRD-TP Washington, D.C. 20315
1	Commander U.S. Army Materiel Command ATTN: AMCRD-TE Washington, D.C. 20315
1	Commander U.S. Army Materiel Command ATTN: AMCRD-MT Washington, D.C. 20315
1	Commander U.S. Army Materiel Command ATTN: AMCRD-W Washington, D.C. 20315
1	Commander U.S. Army Aviation Systems Command ATTN: AMSAV-E 12th & Spruce Streets St. Louis, Missouri 63166
1	Director U.S. Army Air Mobility Research and Development Laboratory Ames Research Center Moffett Field, California 94035
2	Commander U.S. Army Electronics Command ATTN: AMSEL-CE AMSEL-RD Fort Monmouth, New Jersey 07703
2	Commander U.S. Army Missile Command ATTN: AMSMI-R AMSMI-RBL Redstone Arsenal, Alabama 35809
2	Commander U.S. Army Missile Command ATTN: AMSMI-RDK Mr. R. Becht Mr. R. Deep Redstone Arsenal, Alabama 35809
1	Commander U.S. Army Tank-Automotive Command ATTN: AMSTA-RHFL Warren, Michigan 48090
2	Commander U.S. Army Mobility Equipment Research & Development Center ATTN: Tech Docu Cen, Bldg. 315 AMSME-RZT Fort Belvoir, Virginia 22060
2	Commander U.S. Army Munitions Command ATTN: AMSMU-RE AMSMU-RE-M Dover, New Jersey 07801

DISTRIBUTION LIST

No. of Copies	Organization
5	Commander U.S. Army Frankford Arsenal ATTN: SMUFA-U2100 Mr. J. Mitchell SMUFA-U3100 Mr. S. Fulton SMUFA-U3300 Mr. S. Hirshman SMUFA-U3300 Mr. A. Cianciosi L4100-150-2 Mr. C. Sleischer, Jr. Philadelphia, Pennsylvania 19137
1	PLASTEC U.S. Army Picatinny Arsenal ATTN: SMUPA-FR-M-D Dover, New Jersey 07801
7	Commander U.S. Army Picatinny Arsenal ATTN: SMUPA-DR-D Mr. S. Wasserman SMUPA-DR-V, Mr.A.Loeb Mr. D. Mertz SMUPA-D, Mr. Lindner SMUPA-V, Mr. E. Walbrecht Mr. S. Verner SMUPA-VE, Dr. Kaufman Dover, New Jersey 07801
4	Commander U.S. Army Weapons Command ATTN: AMSWE-RE AMSWE-RES AMSWE-RDF AMCPM-RS Rock Island, Illinois 61202
1	Commander U.S. Army Watervliet Arsenal Watervliet, New York 12189
1	Commander U.S. Army Safeguard Systems Command Huntsville, Alabama 35804
1	Director U.S. Army Advanced Materiel Concepts Agency 2461 Eisenhower Avenue Alexandria, Virginia 22314
1	Commander U.S. Army Harry Diamond Laboratories ATTN: AMXDO-TD/002 Washington, D.C. 20438
1	Commander U.S. Army Materials and Mechanics Research Center ATTN: AMXMR-ATL Watertown, Massachusetts 02172
1	Commander U.S. Army Natick Laboratories ATTN: AMXRE, Dr. D. Seiling Natick, Massachusetts 01762
1	Deputy Assistant Secretary of the Army (R&D) ATTN: Mr. C. L. Poor Washington, D.C. 20310
1	Commander U.S. Army Research Office (Durham) ATTN: CRD-AA-EH Box CM, Duke Station Durham, North Carolina 27706

DISTRIBUTION LIST

No. of Copies	Organization
1	Director U.S. Army Advanced Ballistics Missile Defense Agency P. O. Box 1500 Huntsville, Alabama 35809
3	Commander U.S. Naval Air Systems Command ATTN: AIR-604 Washington, D.C. 20360
3	Commander U.S. Naval Ordnance Systems Command ATTN: ORD-9132 Washington, D.C. 20360
2	Commander & Director U.S. Naval Ship Research and Development Center ATTN: Tech Lib Aerodynamic Lab Washington, D.C. 20007
3	Commander U.S. Naval Weapons Center ATTN: Code 753, Tech Lib Code 50704, Dr. W. Haseltine Code 3007, Mr. A. Rice China Lake, California 93555
4	Commander U.S. Naval Ordnance Laboratory ATTN: Code 031, Dr. K. Lobb Code 312, Mr. R. Regan Mr. S. Hastings Code 730, Tech Lib Silver Spring, Maryland 20910
4	Director U.S. Naval Research Laboratory ATTN: Tech Info Div Code 7700, Dr. A. Kolb Code 7720, Dr. E. McClean Mr. I. Vitkovitsky Washington, D.C. 20390
3	Commander U.S. Naval Weapons Laboratory ATTN: Code GX, Dr. W. Kemper Code V213, Mr. J. Edwards Code MAS, Mr. M. Jones Dahlgren, Virginia 22448
2	Commander U. S. Naval Ordnance Station Indian Head, Maryland 20640
1	AEDC (AER) Arnold AFS Tennessee 37389
2	ADTC (ADBPS-12) Eglin AFB Florida 32542
1	AFATL (DLR) Eglin AFB Florida 32542
1	AFATL (DLRD) Eglin AFB Florida 32542
1	AFATL (DLRV) Eglin AFB Florida 32542
2	AFATL (DLRA, Mr. F. Burgess; Tech Lib) Eglin AFB Florida 32542

DISTRIBUTION LIST

No. of Copies	Organization
1	AFWL (WLIL) Kirtland AFB New Mexico 87117
1	ARD (ARIL) Wright-Patterson AFB Ohio 45433
1	ARL Wright-Patterson AFB Ohio 45433
1	ASD (ASBEE) Wright-Patterson AFB Ohio 45433
1	RTD (FEFE, Mr. Sedderke) Wright-Patterson AFB Ohio 45433
1	Director National Bureau of Standards ATTN: Tech Lib U.S. Department of Commerce Washington, D.C. 20234
1	Headquarters National Aeronautics & Space Administration ATTN: Code EP, Mr. Adams Washington, D.C. 20546
1	Director NASA Scientific & Technical Information Facility ATTN: SAK/DL P. O. Box 33 College Park, Maryland 20740
2	Director National Aeronautics & Space Administration George C. Marshall Space Flight Center ATTN: MS-I, Lib R-AERO-AE, Mr. A. Felix Huntsville, Alabama 35812
1	Director Jet Propulsion Laboratory ATTN: Tech Lib 4800 Oak Grove Drive Pasadena, California 91103
1	Director National Aeronautics & Space Administration Langley Research Center ATTN: MS 185, Tech Lib Langley Station Hampton, Virginia 23365
1	Director National Aeronautics & Space Administration Lewis Research Center ATTN: MS 60-3, Tech Lib 21000 Brookpark Road Cleveland, Ohio 44135
2	ARO, Inc. ATTN: Tech Lib Arnold AFS Tennessee 37389
1	Sandia Corporation ATTN: Aerodynamics Dept Org 9320, Mr. R. Maydew P. O. Box 5800 Albuquerque, New Mexico 87115

DISTRIBUTION LIST

No. of Copies	Organization
1	California Institute of Technology Aeronautics Department ATTN: Prof. H. Liepmann Pasadena, California 91102
1	Guggenheim Aeronautical Laboratory California Institute of Technology ATTN: Tech Lib Pasadena, California 91104
3	Cornell Aeronautical Laboratory, Inc. ATTN: Mr. J. Martin Dr. W. Wurster Dr. G. Skinner P. O. Box 235 Buffalo, New York 14221
1	Director Applied Physics Laboratory The Johns Hopkins University 8621 Georgia Avenue Silver Spring, Maryland 20910
1	Massachusetts Institute of Technology Department of Aeronautics & Astronautics ATTN: Tech Lib 77 Massachusetts Avenue Cambridge, Massachusetts 02139
2	University of Michigan Department of Aeronautical Engineering ATTN: Dr. A. Kuethe Dr. M. Sichel East Engineering Bldg. Ann Arbor, Michigan 48104
1	Director Guggenheim Aerospace Labs New York University New York Heights New York, New York 10053
1	Ohio State University Department of Aeronautics & Astronautical Engineering ATTN: Tech Lib Columbus, Ohio 43210
1	Director Forrestal Research Center Princeton University Princeton, New Jersey 08540
	Aberdeen Proving Ground
	Ch, Tech Lib Marine Corps Ln Ofc CDC Ln Ofc CO, USALWL CO, USASASA (2 cys) Dep Press USAMCBD CG, USATECOM ATTN: AMSTE-BE, Mr. Morrow AMSTE-TA-R, Mr. Wise

Unclassified

Security Classification

DOCUMENT CONTROL DATA · R & D

(Security classification of title, body of abstract and indexing annotation must be entered when the overall report is classified)

1. ORIGINATING ACTIVITY (Corporate author)	2a. REPORT SECURITY CLASSIFICATION
U. S. Army Ballistic Research Laboratories Aberdeen Proving Ground, Maryland 21005	Unclassified
	2b. GROUP

3. REPORT TITLE

VACUUM ULTRAVIOLET RADIATION IN THE EXPANSION TUBE

4. DESCRIPTIVE NOTES (Type of report and inclusive dates)

5. AUTHOR(S) (First name, middle initial, last name)

Fritz H. Oertel, Jr.

6. REPORT DATE	7a. TOTAL NO. OF PAGES	7b. NO. OF REFS
November 1972	31	18

8a. CONTRACT OR GRANT NO.	9a. ORIGINATOR'S REPORT NUMBER(S)
b. PROJECT NO. RDT&E 1T061102A33D	BRL MEMORANDUM REPORT NO. 2249
c.	9b. OTHER REPORT NO(S) (Any other numbers that may be assigned this report)
d.	

10. DISTRIBUTION STATEMENT

Approved for public release; distribution unlimited.

11. SUPPLEMENTARY NOTES	12. SPONSORING MILITARY ACTIVITY
	U. S. Army Materiel Command Washington, D. C.

13. ABSTRACT

The findings are presented of an optical survey of vacuum ultraviolet (VUV) radiation emitted from the shock layer of a 1-1/2" diameter sphere in hypersonic flows of air, argon, nitrogen and argon-nitrogen mixtures. Free stream velocities of 17,000-20,000 ft/sec and densities corresponding to altitudes ∿ 90,000 ft. were obtained in the BRL expansion tube facility; steady flow conditions prevailed over the model for about 75 μsec. The radiation was recorded on sensitized film down to a lower limit of 1100 Å. The purpose of the survey was to explore the feasibility of using this facility to measure time and space resolved radiation of the nonequilibrium, vibrationally-excited N_2 in the shock layer; part of this radiation is conjectured to ionize O_2 ahead of the shock around a hypersonic vehicle, thus enhancing its radar signature. Methods and problems of measuring VUV from this shock layer are discussed.

DD FORM 1 NOV 68 1473 REPLACES DD FORM 1473, 1 JAN 64, WHICH IS OBSOLETE FOR ARMY USE.

Unclassified

Security Classification

14. KEY WORDS	LINK A		LINK B		LINK C	
	ROLE	WT	ROLE	WT	ROLE	WT
Radiation						
Vacuum Ultraviolet						
Expansion Tube						
Nonequilibrium						
Photoionization						
Vacuum Monochromator/Spectrograph						